Available online at www.sciencedirect.com
SCIENCE DIRECT®
International Journal of Thermal Sciences 45 (2006) 16–28
International Journal of Thermal Sciences
www.elsevier.com/locate/ijts

Convective heat and mass transfer with evaporation of a falling film in a cavity

S. Ben Jabrallah [a,b], A. Belghith [b], J.P. Corriou [c,*]

[a] *Faculté des Sciences de Bizerte, 7021 Bizerte, Tunisia*
[b] *Faculté des Sciences de Tunis, Laboratoire des Transferts de Chaleur et de Masse, Campus Universitaire, 1060, Tunisia*
[c] *Laboratoire des Sciences de Génie Chimique, CNRS-ENSIC, 1 rue Grandville BP 451, 54001 Nancy cedex, France*

Received 26 November 2004; received in revised form 2 May 2005; accepted 10 May 2005

Available online 8 June 2005

Abstract

The heat and mass transfer involved in the evaporation of a water falling film in a closed rectangular cavity of geometric form factor equal to 10 is studied numerically and experimentally. The wall which supports the liquid film is heated by a constant heat flux. The vapor thus formed is condensed on the opposite wall maintained at a constant and uniform temperature. The study objective is a better understanding of the evaporation phenomenon in order to improve the yield. A numerical model has been built from the conservation equations in the gas and liquid phases. The main characteristic of the present study is the way of treating the transfer in the liquid film. A method based on the mass and heat balances has been developed where the balances are obtained by integration of the mass and energy conservation equations over small height increments. This method allows us to avoid the explicit solution of the momentum and energy equations which is more difficult because of the presence of a fabric material placed on the heated wall to stabilize the liquid film. The obtained results allow us to describe the thermodynamic state of the heated film by means of the liquid temperature and evaporation flow rate. The heated film presents two zones: a heating zone located near the inlet of the cavity and an evaporation zone which covers the rest of the wetted surface. The extent of this effective surface of evaporation has been studied with respect to the operating parameters: on the one hand, the heat flux and the temperature of the condensation wall that in general depend on the climatic conditions, on the other hand, the water feed temperature and flow rate that can be varied by the user and act directly on the liquid film. The influence of the two latter parameters on the exchanges at the liquid–gas interface has been characterized in terms of local Sherwood and Nusselt numbers.

Résumé

Nous étudions les transferts de chaleur et de matière qui accompagnent l'évaporation d'un film d'eau tombant dans une cavité rectangulaire fermée de facteur de forme géométrique égal à 10. La paroi qui supporte le film liquide est chauffée à flux constant. La vapeur qui se forme au niveau de la paroi mouillée se condense sur la paroi opposée maintenue à température uniforme. L'étude vise une meilleure compréhension du phénomène d'évaporation afin d'en améliorer le rendement. Un modèle numérique a été construit à partir des équations de conservation dans les phases gazeuse et liquide. La particularité de cette étude réside dans la manière de traiter les transferts dans le film liquide. Nous avons développé une méthode basée sur les bilans massique et thermique obtenus par intégration des équations de conservation de matière et d'énergie sur de faibles incréments de hauteur. Cette méthode permet d'éviter la résolution explicite des équations de quantité de mouvement et d'énergie rendue plus difficile par la présence d'un tissu qui sert à maintenir le film liquide. Les résultats obtenus ont permis de décrire l'état thermodynamique du film chauffé à l'aide de la température du liquide et du débit d'évaporation. Le film chauffé présente deux zones : une zone d'échauffement située près de l'entrée de la cavité et une zone d'évaporation qui couvre le reste de la surface mouillée. L'étendue de cette surface effective d'évaporation a été étudiée en fonction des paramètres opératoires : d'une part la densité du flux de chauffage et la température de la paroi de condensation qui dépendent en général des conditions climatiques, d'autre part la température et le débit massique

* Corresponding author.
E-mail address: corriou@ensic.inpl-nancy.fr (J.P. Corriou).

1290-0729/$ – see front matter
doi:10.1016/j.ijthermalsci.2005.05.001

de l'eau d'alimentation qui peuvent être choisis par l'utilisateur et agissent directement sur le film liquide. L'influence de ces deux derniers paramètres sur les échanges à l'interface liquide–gaz a été caractérisée par les nombres locaux de Sherwood et de Nusselt.

Keywords: Evaporation; Desalination; Falling film; Salted water; Natural convection

1. Introduction

Heat transfer through a thin film with evaporation poses many theoretical problems and presents a great practical interest. Thin films find applications in industrial processes: the heat coefficients occurring are large for small deviations between the wall temperature and the saturation temperature of the liquid film. According to the application, the concern is the drying of the film and thus its evaporation (in case of mass transfer) or the cooling of the wall (in case of heat transfer). With respect to evaporation, thin films are met in heat exchangers, in cooling, petroleum refining, thermal protection of heated walls, food industry, etc., while other applications concern film evaporation in desalination processes that use salted water distillation in an enclosure. The process is based on humidification and dehumidification of air at low temperature, inside a cavity. First, water evaporates at the free surface of a liquid film falling along the internal face of a heated wall. The vapor is transported by natural convection flow. On the opposite wall, maintained at a temperature lower than the saturation temperature, a fraction of the steam contained in the gas mixture is condensed.

Most works deal with evaporation of a liquid film in an open space like a plane plate in air [1] or half confined like in the case of a parallel plate channel [2,3] or a tube [4]. Studies concerning evaporation in an enclosure are less common. However this configuration is often met in distillation systems used for desalination.

The difficulty of the study of the evaporation of a liquid film is related to the coupling of the liquid and gas phases and to the complexity of the occurring phenomena. Actually, the thickness of the liquid film is very low while the falling liquid overcomes very important thermal exchanges due to the heating and to evaporation. For those reasons, we have particularly studied the phenomena concerning the liquid film.

Studies concerning the evaporation of a liquid film differ in particular by the way of taking into account the heat and mass transfer in the liquid film and its interaction with the neighbouring gas. The first works such as Chow and Chung [5], Schröppel and Thiele [6], supposed that the liquid film is stagnant. The equations ruling the transfer in the liquid are thus reduced to the boundary conditions used for the solving of the equations of the gas phase. However this approach does not allow us to consider some characteristics of the falling liquid film, in particular its inlet flow rate.

A one-dimensional formulation has been proposed by Shembharkar and Pai [7], Baumann and Thiele [8], who neglected the inertial terms in the momentum and the convective terms in the energy equation. They applied this method to incorporate the influence of the transfer in a liquid film of refrigerant flowing on a plate and submitted to a stream of hot gas in a turbulent flow.

To improve this analysis, authors as Tsay et al. [9], Yan and Lin [10], Yan and Soong [1], presented a partly two-dimensional modelling. In the liquid film, they neglect the inertial terms in the momentum equation and the convective transport term along the direction perpendicular to the wall. That amounts to describe the heat and mass transfer in the liquid phase by a one-dimensional momentum equation and a two-dimensional heat equation.

Recently, Cherif and Daif [11], Agunaoun et al. [12], Mezaache and Daguenet [13] considered two-dimensional equations in the liquid film. In this way, Agunaoun et al. [12] applied this method to study the evaporation of a thin water film in a stream of humid air flowing on a plane inclined surface at constant temperature larger than the air temperature. They have represented the evolution of the evaporated mass fraction along the wall equal to the ratio of the evaporated flux by the mass flow rate of the liquid film at the inlet. As they considered large lengths for the plane, they determined the dried length and showed that it depends on the properties of the air flow, mainly its velocity and its steam concentration. Cherif and Daif [11] adopted a two-dimensional model to perform a numerical analysis on the heat and mass transfer between two plane parallel plates in presence of a binary liquid film falling on one heated plate. They examined the influence of the film thickness by comparing the different studies that use a simplified model. They concluded that the results obtained by neglecting the liquid film can be erroneous by more than 1000%. The evaporation of a water falling film on an inclined plate in a laminar stream of humid air has been studied numerically by Mezaache and Daguenet [13]. The gas and liquid phase equations have been considered under a two-dimensional form. These authors showed that the enthalpy diffusion term can be neglected in the heat equation for the gas phase. However the essential result of their study is the following:

- when the wall is adiabatic, the liquid flow rate has no influence on the heat and mass transfer in the film and the one-dimensional model can be used,
- when the wall is isothermal or crossed by a heat flux, three cases are possible:
  - if the flow rate is smaller than 10^{-3} kg·m^{-1}·s^{-1}, the one-dimensional model is sufficient,

Nomenclature

b	cell width (distance between vertical plates)	m
C	molar concentration of water vapor	$\text{mol}\cdot\text{m}^{-3}$
C_s	concentration of saturating vapor	$\text{mol}\cdot\text{m}^{-3}$
c_p	heat capacity at constant pressure	$\text{J}\cdot\text{kg}^{-1}\cdot\text{K}^{-1}$
D	diffusivity of water vapor in air	$\text{m}^2\cdot\text{s}^{-1}$
h	cell height	m
H	form factor of the cell	
l	length of the water film	m
L_v	latent heat of water	$\text{J}\cdot\text{kg}^{-1}$
M	molecular weight	$\text{kg}\cdot\text{mol}^{-1}$
$\dot{m}$	mass flow rate of water per unit width	$\text{kg}\cdot\text{m}^{-1}\cdot\text{s}^{-1}$
$\dot{m}_{\text{in}}$	mass flow rate of feed water per unit width	$\text{kg}\cdot\text{m}^{-1}\cdot\text{s}^{-1}$
$\dot{m}_v$	mass flux evaporated at the interface	$\text{kg}\cdot\text{m}^{-2}\cdot\text{s}^{-1}$
$\dot{m}_s$	mass flow rate of the salted water evacuated per unit width	$\text{kg}\cdot\text{m}^{-1}\cdot\text{s}^{-1}$
p	pressure	Pa
$\dot{q}_f$	heat flux to the water film	$\text{W}\cdot\text{m}^{-2}$
$\dot{q}_{\text{cd}}$	heat flux exchanged between vertical plates by conduction	$\text{W}\cdot\text{m}^{-2}$
$\dot{q}_{\text{cv}}$	heat flux exchanged at the interface by convection	$\text{W}\cdot\text{m}^{-2}$
$\dot{q}_l$	latent heat flux	$\text{W}\cdot\text{m}^{-2}$
S_v	ratio of the effective evaporation area by the total area of the liquid film	
T	temperature	K or °C
T_{in}	temperature of water feed	K or °C
T_w	mean temperature of water in the film at height y	K or °C
u, v	components of velocity	$\text{m}\cdot\text{s}^{-1}$
w	mass fraction of water vapor	
(x, y)	Cartesian coordinates	m
(X, Y)	dimensionless coordinates	

Greek symbols

β_m	mass expansion coefficient	$\text{m}^3\cdot\text{mol}^{-1}$
β_T	thermal expansion coefficient	K^{-1}
δ	thickness of the water film	m
η	yield of the distillation cell	
λ	thermal conductivity	$\text{W}\cdot\text{m}^{-1}\cdot\text{K}^{-1}$
μ	dynamic viscosity	Pa·s
ν	cinematic viscosity	$\text{m}^2\cdot\text{s}^{-1}$
ρ	density of the gas mixture	$\text{kg}\cdot\text{m}^{-3}$

Subscripts

a	air
c	reference (at the condensation plate)
δ	liquid–gas interface
g	gas phase
sat	saturation
v	water vapor
w	water

– if the flow rate is included in the interval $[10^{-3}, 10^{-2}]$ $\text{kg}\cdot\text{m}^{-1}\cdot\text{s}^{-1}$, the partially two-dimensional model is usable,
– if the flow rate is larger than 10^{-2} $\text{kg}\cdot\text{m}^{-1}\cdot\text{s}^{-1}$, the two-dimensional model must be used.

It appears clearly that the consideration of the heat and mass transfer inside the liquid film complicates the study of the evaporation phenomenon. The difficulty resides in two points:

- the coupling of the liquid and gas phases. However, the simplest hypothesis is that recommended by Nusselt [14,15] who assumed that the shear stress is zero at the liquid–vapor interface

$$\frac{\partial v}{\partial x} = 0$$

which allows us to decouple the liquid and vapor phases at the hydrodynamic level. More recently, this hypothesis has been replaced by the continuity of the shear stress at the interface expressed by Eq. (13).
- taking into account the two-dimensional character of the flow equations in the liquid phase poses several problems essentially related to the very low thickness of the film with respect to the system dimensions and induces heavy computation.

In the study of coupled evaporation and condensation in a distillation cell, this difficulty is increased as the evaporation occurs in a confined space. The present work is motivated by the search of a simple and efficient method allowing us to describe the thermodynamic state of the evaporating film in a closed rectangular cavity and to predict the evaporated flux.

In a previous article [16], we studied the coupled heat and mass transfer in a rectangular enclosure with application to a distillation cell. The vertical wall where the liquid film falls is submitted to a constant and homogeneous heat flux while the opposite wall is maintained at a constant temperature. In the numerical study, we developed a method allowing us to take into account the changes of the thickness of the liquid film without explicitly solving the flow equations for the liquid. In parallel, we performed an experimental work to compare the results concerning mainly the mean global distillation flow rate. The present work deals with the behaviour of the liquid film in a similar configuration and aims at describing its thermodynamic state by studying the maps of its mean temperature and of the evaporation ratio.

2. Problem position

The objective is to model the behaviour of a distillation cell whose geometric form can be represented by a rectangular cavity having a high form factor. Fig. 1 describes the cell with its geometric parameters.

The cavity (Fig. 1) is a parallelepiped of low width b, formed by an adiabatic frame of height h, length l, closed on both sides by two vertical square plates, of dimension 0.4 m × 0.4 m, distant of b. On the internal face of the plate heated by a constant heat flux, a very thin water film flows with a thickness depending on the vertical position.

The constant heating of the plate enables to first increase the temperature of the falling water film, then to evaporate part of it. The water film enters with a mass flow rate per unit width $\dot{m}_{\text{in}}$, and leaves the cell with a mass flow rate $\dot{m}_s$. The opposite plate is maintained at constant temperature T_c. The existence of temperature and concentration gradients creates a movement of the mixture air–water vapor inside the cavity. On contact with the opposite plate, maintained at temperature T_c, a part of water vapor condensates. On the other hand, the condensation on the heated film is neglected. Such a cavity may represent a stage of a distillation unit composed of several cells in series [17].

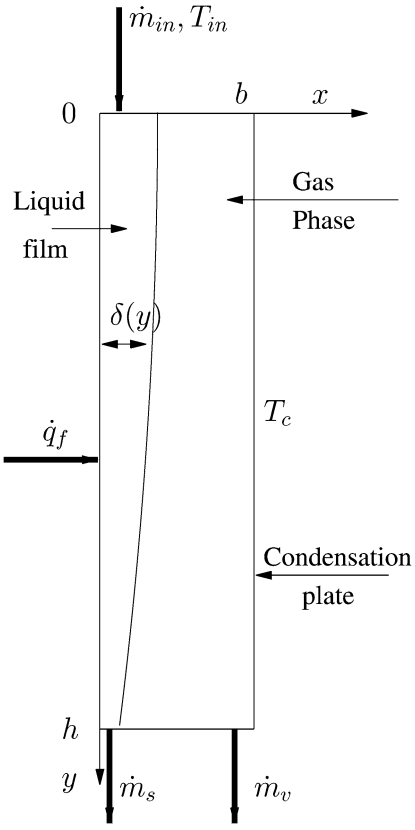

Fig. 1. Scheme of the distillation cell.

3. Fundamental equations

3.1. In the liquid film

With respect to the liquid film that falls along the wall, it is assumed that the flow is laminar and that the inertia term is negligible. The momentum equation (Yan and Lin [10]) is

$$\frac{\partial}{\partial x}\left(\mu_w \frac{\partial v_w}{\partial x}\right) + \rho_w g = 0 \tag{1}$$

Taking into account the approximations of the limit layer, the energy equation is

$$\rho_w c_p u_w \frac{\partial T_w}{\partial y} = \frac{\partial}{\partial x}\left(\lambda_w \frac{\partial T_w}{\partial x}\right) \tag{2}$$

where the right member expresses the conductive transport. In the two previous equations, the film being vertical, the convective transport is reduced to the term with respect to y direction.

3.2. In the gas phase

In the gas phase, the flow is studied as two-dimensional and considered to be laminar. Only the steady-state case is modelled. Boussinesq hypothesis is admitted. All the other physical properties of the fluid are updated at each time iteration and calculated at the mean temperature of the fluid in the considered phase. The viscous dissipation is negligible. The pressure terms are neglected in the energy balance. The secondary Dufour and Soret effects are supposed to be negligible and the concentration of the diffusing species remains low.

The previous hypotheses being given, the movement of the fluid mixture air–water vapor inside the cavity can be described by the conservation equations:

Continuity equation

$$\frac{\partial u}{\partial x} + \frac{\partial v}{\partial y} = 0 \tag{3}$$

u and v-momentum equations

$$\rho u \frac{\partial u}{\partial x} + \rho v \frac{\partial u}{\partial y} = -\frac{\partial p}{\partial x} + \mu\left(\frac{\partial^2 u}{\partial x^2} + \frac{\partial^2 u}{\partial y^2}\right) \tag{4}$$

$$\rho u \frac{\partial v}{\partial x} + \rho v \frac{\partial v}{\partial y} = -\frac{\partial p}{\partial y} + \rho g + \mu\left(\frac{\partial^2 v}{\partial x^2} + \frac{\partial^2 v}{\partial y^2}\right) \tag{5}$$

Energy equation

$$\rho c_p\left(u\frac{\partial T}{\partial x} + v\frac{\partial T}{\partial y}\right) = \lambda\left(\frac{\partial^2 T}{\partial x^2} + \frac{\partial^2 T}{\partial y^2}\right) + \rho D(C_{\text{pv}} - C_{\text{pa}})\frac{\partial T}{\partial x}\frac{\partial w}{\partial x} \tag{6}$$

Transport of the diffusing species equation

$$u\frac{\partial w}{\partial x} + v\frac{\partial w}{\partial y} = D\left(\frac{\partial^2 w}{\partial x^2} + \frac{\partial^2 w}{\partial y^2}\right) \tag{7}$$

4. Boundary conditions

4.1. For the liquid film

The stream of water that must fall along the internal face of the heated plate enters the cell according to a uniform profile with a mass flow rate $\dot{m}_{\text{in}}$ and a temperature T_{in}

$$\dot{m} = \dot{m}_{\text{in}}, \qquad T_w = T_{\text{in}} \quad \text{at } y = 0 \tag{8}$$

where T_w represents the mean temperature of the water film at the considered height. At steady state, it is assumed that the heat flux absorbed by the external face is totally transmitted to the liquid film which flows on its internal face, giving the condition

$$-\lambda_w \left(\frac{\partial T_w}{\partial x} \right) = \dot{q}_f \quad \text{at } x = 0 \tag{9}$$

The following condition of adherence of the liquid at the internal face of the metal plate is

$$v_w = 0 \quad \text{at } x = 0 \tag{10}$$

4.2. At the liquid–gas interface

The hypothesis of continuity of velocity and temperature at the interface ($x = \delta$) allows us to write

$$v_w(\delta) = v(\delta), \qquad T_w(\delta) = T(\delta) \tag{11}$$

The transverse velocity of the air–vapor mixture can be expressed as Tsay and Lin [18]

$$u(\delta) = -\frac{D}{(1 - w_\delta)} \left(\frac{\partial w}{\partial x} \right)_\delta \tag{12}$$

The continuity equation for the shear stresses, according to Tsay et al. [9], Mezaache and Daguenet [13], can be written as

$$\mu_w \left(\frac{\partial v_w}{\partial x} \right)_\delta = \mu_g \left(\frac{\partial v}{\partial x} \right)_\delta \tag{13}$$

The continuity of the heat flux at the interface is given by

$$-\lambda_w \left(\frac{\partial T_w}{\partial x} \right)_\delta = -\lambda_g \left(\frac{\partial T}{\partial x} \right)_\delta + L_v \dot{m}_v \tag{14}$$

In this latter equation, the mass flux $\dot{m}_v$ exchanged at the interface is given by applying Fick law (Tsay and Lin [18]), and supposing that the interface is impermeable to dry air, resulting in

$$\dot{m}_v = -\frac{\rho_g D}{1 - w_\delta} \left(\frac{\partial w}{\partial x} \right)_\delta \tag{15}$$

where w_δ is the mass fraction of water vapor at the interface, D is the diffusion coefficient of water in air.

4.3. In the gas phase

The walls at $y = 0$ and $y = h$ are considered adiabatic

$$\left(\frac{\partial T}{\partial y} \right)_{y=0} = \left(\frac{\partial T}{\partial y} \right)_{y=h} = 0 \quad \text{for } \delta \leqslant x \leqslant b \tag{16}$$

The condensation plate is maintained at constant temperature T_c

$$T = T_c \quad \text{at } x = b \tag{17}$$

The condition of adherence at the lower and upper walls gives

$$u = v = 0 \quad \text{at } y = 0 \quad \text{and}$$
$$y = h \quad (\text{with } \delta \leqslant x \leqslant b) \tag{18}$$
$$u = v = 0 \quad \text{at } x = b \tag{19}$$

The thermodynamic equilibrium is assumed during the change of phase

$$w(\delta) = w_{\text{sat}}(T_\delta) \quad \text{at } x = \delta \tag{20}$$
$$w(b) = w_{\text{sat}}(T_c) \quad \text{at } x = b \tag{21}$$

5. Solution method

The equations describing the fluid flow inside the cavity have been discretized according to the finite volume method [19]. Each equation results in a linear set of equations which is transformed as a tridiagonal set of equations according to the horizontal and vertical directions. To solve it, the method of double sweeping was adopted. This method has the advantage to quickly propagate the influence of the boundary conditions towards the inner domain, and consequently, to accelerate the convergence. To calculate the thermodynamic properties of the air–water mixture, the influence of water vapor and the temperature available at each iteration have been taken into account [20]. In their study of the evaporation of a water falling film on an inclined plate, Mezaache and Daguenet [13] have shown that the enthalpy diffusion term does not influence the film temperature and consequently the variables that depend on it. It results that the corresponding second right-hand term of Eq. (6) can be neglected.

To describe the flow and the temperature distribution in the liquid film, a method based on the mass and energy balances at each level defined by the discretization grid in the gas phase was developed [16].

At height y, instead of determining the individual changes of the flow velocity u_w and of the thickness $\delta(y)$ of the film, the mass flow rate by unit of length

$$\dot{m}(y) = \rho_w u_w \delta(y) \tag{22}$$

has been determined by integration of the energy equation between the heights y and $y + \mathrm{d}y$. The mass balance allows us to take into account the variation of the mass flow rate of liquid (Fig. 1). This method presents the advantage to simplify the solving of the equations while allowing us to determine the distributions of temperature and flow rate of the liquid film at a given height y. Furthermore in actual practice, in the present study, a thin cotton tissue has been used to maintain the liquid film against the heated wall.

The presence of a porous medium in the liquid phase makes more complicated the solving of its dynamics. The developed method, based on local balances, allows us to overcome that difficulty.

The procedure of general solving is iterative. Each iteration consists in solving the set of equations of the gas phase by using the available boundary conditions. In the sequel, the equations resulting from the balances in the liquid film are solved, considering the new distributions of the variables in the gas phase. Thus the boundary conditions as well as the physical properties are updated at each iteration. In this manner, the procedure considers the coupling between the gas and liquid systems. The procedure is repeated until satisfaction of the criterion convergence. The validation of the numerical code and the details of the calculation procedure are described in a previous paper [16].

6. Experimental setup

The experimental setup comprises a distillation cell, a heating device, a cooling device for the condensation wall and a water feeding device (Fig. 2). The distillation cell itself is a parallelepiped cavity, of form factor $H = h/b = 10$, of dimensions: $l = 0.50$ m, $h = 0.50$ m and $b = 0.05$ m. The active walls of the cell which are the vertical walls, between

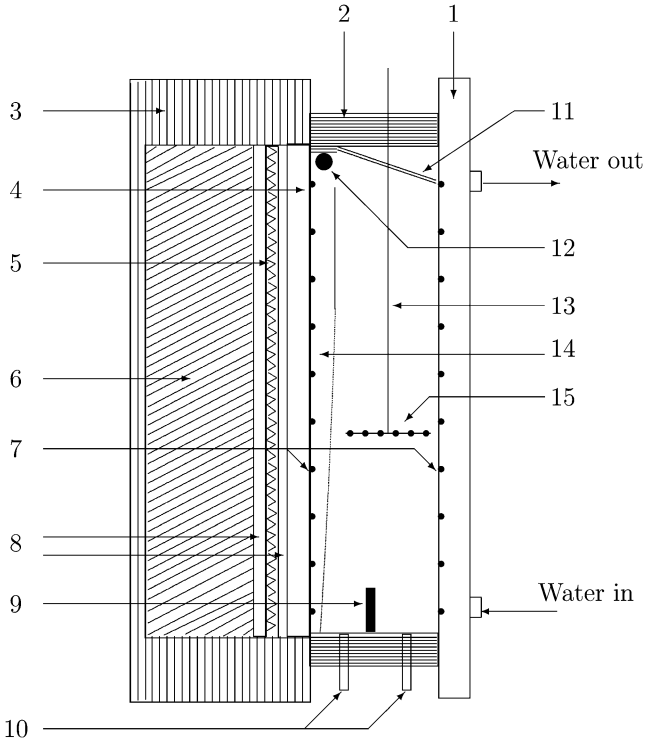

Fig. 2. Experimental setup. 1: Condensation plate. 2: Plexiglas frame. 3: Wood frame. 4: Heated plate. 5: Resistance made of carbon sheets. 6: Heat insulator made of cork. 7: Thermocouples (K-type). 8: Plates of Samicanite electrical insulator. 9: Brine-distillate separation plate. 10: Recovery of brine and distillate. 11: Tilted plate. 12: Duct. 13: Moving rod. 14: Liquid film. 15: Thermocouples (T-type).

which the heat and mass exchange take place, are two square stainless steel plates of thickness 0.01 m, of side 0.50 m. These walls are distant by 0.05 m and separated by a thick Plexiglas frame to reduce the side heat losses.

The wall supporting the film is equipped with the heating system. To realize the condition of imposed heat flux at the wall, an electrical resistance cut in a flexible graphite sheet allows us to uniformly distribute the imposed flux at the evaporation wall. The back face is sufficiently insulated to totally guide the flux towards the face in contact with the film. Supposing that the resistance integrally transforms the electrical power into heat flux by Joule effect, the flux can be varied by acting on the power generator. A water cooling has been machined in the opposite wall to control its temperature and insure its cooling. To realize a low falling film, a very slim fabric has been spread which presents meshes of very small dimension. When wetted, the fabric adheres to the wall by capillarity. Because of the very low thickness of the falling film thus realized, this fabric presents the advantage to reduce the thermal resistance at the wall. The water feeding is ensured by a cylindrical tube perforated along one of its lines and linked to a constant level recipient. The tube, placed at the top of the cell, is surrounded by the fabric in order to form the liquid film.

This setup is completed by the measurement system. Ten chromel–alumel (K-type) thermocouples are disposed according to the height on each on the internal faces of the active walls. Moreover, six copper–constantan (T-type) thermocouples are placed on a rod perpendicular to the active walls to measure the gas mixture temperature inside the cavity. This rod can move vertically in order to obtain the temperatures at different levels of the cavity. A typical experiment consists in imposing a heat flux while fixing the flow rate, the temperature of the feed water and the temperature of the condensation wall. When the steady-state regime is obtained, the temperature of the liquid film is measured along the heated wall as well as the distillate flow rate. The temperature acquisition is automated by means of an interface card and a microcomputer. The thermocouples of the heated wall are placed along the wetted face. As the film is very thin, it can be considered that the measurement indicates the mean equilibrium temperature at the solid–liquid interface and can be compared to the calculated temperature T_w. The thermocouples have been calibrated using a micro-controlled temperature thermostat and a digital thermometer and the overall accuracy is believed to be within 0.2 °C. Their time response is below 5 s. Due to the automated data acquisition system, the reproducibility is around 0.1 °C. For the flow rate measurement, a balance with a sensitivity of 10^{-4} kg records the cumulated distillated mass.

7. Validation of the numerical code

The evaporation of the liquid film plays an important rôle in the yield of a distillation cell defined as the ratio of the

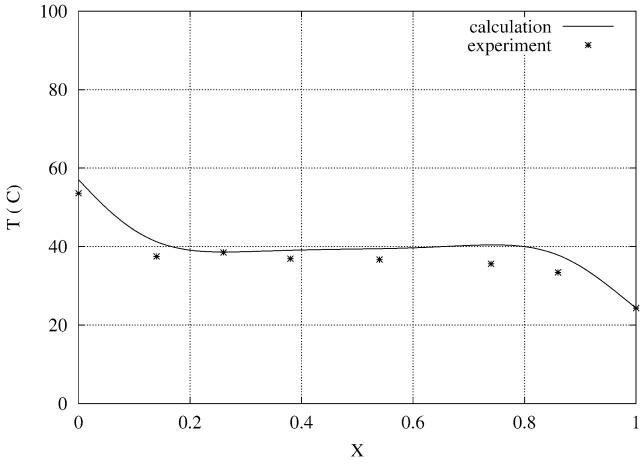

Fig. 3. Comparison of the experimental and calculated temperature profiles in the cavity at $y = h/2$ (conditions: $T_c = 24.3\,^{\circ}\mathrm{C}$, $T_{\mathrm{in}} = 33.7\,^{\circ}\mathrm{C}$, $\dot{m}_{\mathrm{in}} = 0.811 \times 10^{-3}\ \mathrm{kg{\cdot}s^{-1}{\cdot}m^{-1}}$, $\dot{q}_f = 700\ \mathrm{W{\cdot}m^{-2}}$).

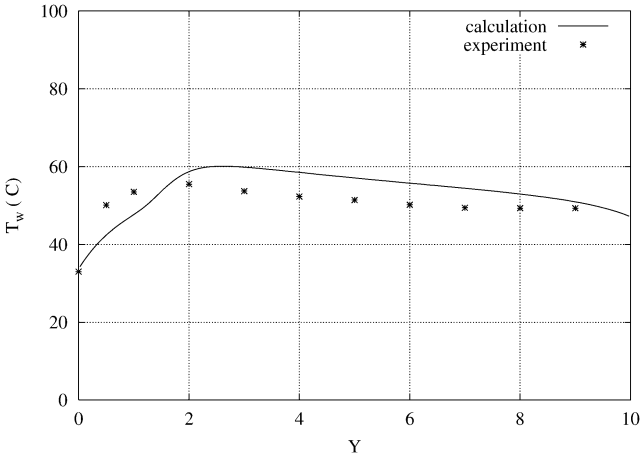

Fig. 4. Comparison of the experimental and calculated temperature profiles along the heated wall (conditions: $T_c = 24.3\,^{\circ}\mathrm{C}$, $T_{\mathrm{in}} = 33.7\,^{\circ}\mathrm{C}$, $\dot{m}_{\mathrm{in}} = 0.811 \times 10^{-3}\ \mathrm{kg{\cdot}s^{-1}{\cdot}m^{-1}}$, $\dot{q}_f = 700\ \mathrm{W{\cdot}m^{-2}}$).

heat flux used in actual evaporation to the heat flux applied at the heated wall

$$\eta = \frac{\dot{m}_v L_v}{\dot{q}_f} \tag{23}$$

The objective of the present study is to realize a numerical simulation of the behaviour of a distillation cavity in order to perform a parametric study of the evaporation of the liquid film. The numerical code has to be validated. In this order, a comparison with the numerical results obtained by other searchers was presented in a previous article [16]. In the present work, a comparison with our experimental results is provided.

In a first stage, the comparison dealt with the influence of the gas phase temperature, between the two vertical walls, at a given height. Fig. 3 presents the calculated and measured temperatures of the gas mixture with respect to the abscissa x, at $y = h/2$. Both types of results show that the thermal gradient is large close to the walls, though inside the cavity, the variation is relatively low. The agreement between calculation and experiment is good. However a deviation is observed at $x = 0$, where the calculation gives a value of the liquid–gas interface temperature, though the measurement concerns the mean film temperature at that level, as this latter is effectively given by the thermocouple sticked to the wetted wall.

As the main objective consists in using the numerical results in order to study the evaporation of the liquid film heated in a cavity, it is necessary to validate the simulation of the description of the thermal behaviour of the film. Thus we represented the variation of the liquid film temperature with respect to the height y depicted in Fig. 4 which presents a comparison between experiment and simulation. The difficulty of measuring the temperatures of the thin falling film of thickness below 1 mm must be recalled. The numerical and experimental results show some disagreement, in particular concerning the calculated temperature which seems overestimated on the majority of the film extent, which is due to the adopted hypothesis assuming that the flux applied to the wall is totally transmitted to the film. The deviation observed at the top of the cell can be explained by the instability of the liquid flow in this region, which phenomenon was not considered. However, both lines have the same allure: each one presents a heating zone located at the entrance of the cell, then the liquid film temperature decreases very slowly because of the evaporation on the rest of the surface. Both results are also in correct agreement concerning the position of the maximum temperature, which justifies the use of the code to study the extent of the evaporation surface.

8. Results

The thermodynamic state of the liquid film can be described by the evaporated mass flux $\dot{m}_v$ which depends on the temperature of the liquid–gas interface, or still on the mean temperature of the film T_w at the considered height. Indeed Cherif and Daif [11] showed that the temperature in the liquid film varies little with respect to the transverse coordinate. In order to describe the state of evaporation of the film, the distribution of those variables along the heated wall has been studied, by representing their variations with respect to the dimensionless height $Y = y/b$.

The obtained results show that the falling film presents two zones: one situated close to the inlet of the cavity (corresponding to Y small) where the liquid is simply heated and undergoes very little evaporation. In any zone of the falling film, the energy balance (Fig. 5) for a section of width $\mathrm{d}y$ is

$$\dot{q}_f\,\mathrm{d}y = \dot{m} c_p\,\mathrm{d}T_w + \dot{q}_l\,\mathrm{d}y + \dot{q}_{\mathrm{cv}}\,\mathrm{d}y \tag{24}$$

where $\dot{q}_l$ and $\dot{q}_{\mathrm{cv}}$ are the heat fluxes corresponding respectively to evaporation and convection. In absence of evaporation or condensation: $\dot{q}_l = 0$ and $\dot{m} = \dot{m}_{\mathrm{in}}$, and by noticing that the heat flux exchanged by convection between the liquid film and the gas mixture remains negligible compared to

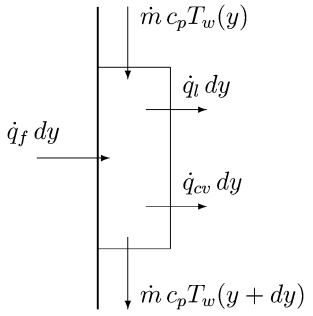

Fig. 5. Energy balances at the liquid film for a finite element.

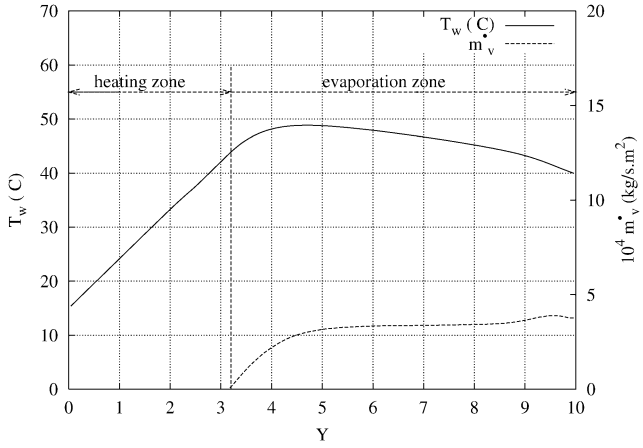

Fig. 6. Description of the thermodynamic state of the liquid film (conditions: $T_c = 16\,^{\circ}\mathrm{C}$, $T_{\mathrm{in}} = 15\,^{\circ}\mathrm{C}$, $\dot{m}_{\mathrm{in}} = 0.833 \times 10^{-3}$ kg·s^{-1}·m^{-1}, $\dot{q}_f = 800$ W·m^{-2}).

the exchanges involved (Ben Jabrallah et al. [16]), this equation becomes

$$\dot{q}_f \,\mathrm{d}y = \dot{m}_{\mathrm{in}} c_p \,\mathrm{d}T_w \quad \text{or} \quad \frac{\mathrm{d}T_w}{\mathrm{d}y} = \frac{\dot{q}_f}{\dot{m}_{\mathrm{in}} c_p} \tag{25}$$

This equality shows that the expression of $\mathrm{d}T_w/\mathrm{d}y$ when $\dot{q}_l = 0$ depends only on the heat flux applied and on the feed flow rate, which explains the linear shape of the plot describing the variation of the mean temperature of the water film with respect to the height y, in the neighborhood of the inlet of the cell corresponding to low Y (Fig. 6).

The second zone of the film is the part of the wetted surface corresponding to high Y where evaporation prevails and where the major part of the heat provided is converted into latent heat. To characterize the evaporation region, the ratio S_v of the real surface of evaporation to the total wetted surface per unit width has been calculated and its variation is studied with respect to the four main parameters that influence the heat and mass transfer in the distillation cell, i.e. the temperature and the flow rate of feed water, the heat flux and the temperature of the condensation plate.

8.1. Influence of the heat flux

The heat flux $\dot{q}_f$ imposed to the heated wall is varied between 200 W·m^{-2} and 1400 W·m^{-2}, corresponding to

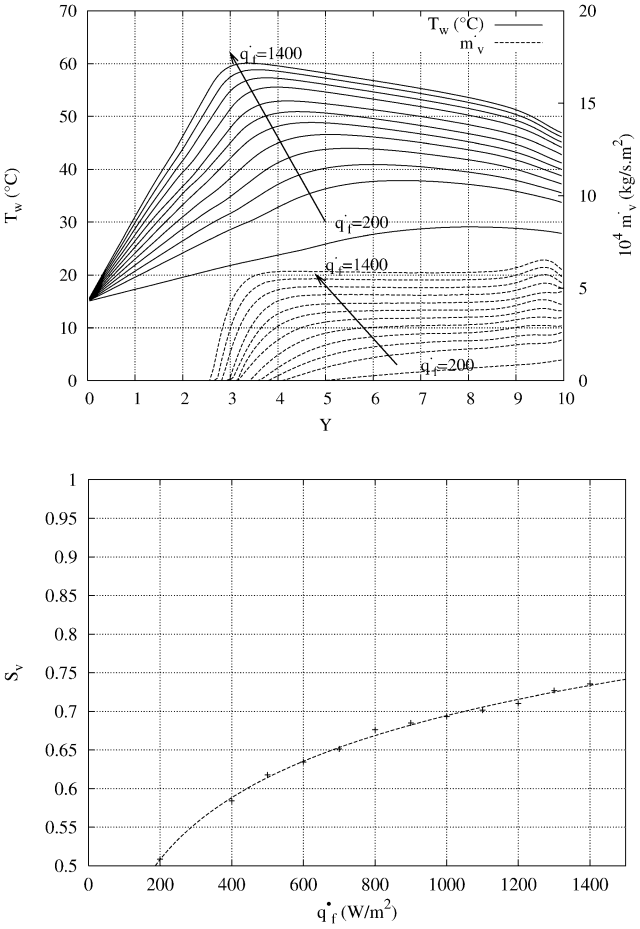

Fig. 7. Influence of the heat flux expressed in W·m^{-2}. Top: profiles of film temperature and evaporated mass flux. Bottom: variation of the fraction of effective evaporation area (conditions: $T_c = 16\,^{\circ}\mathrm{C}$, $T_{\mathrm{in}} = 15\,^{\circ}\mathrm{C}$, $\dot{m}_{\mathrm{in}} = 0.833 \times 10^{-3}$ kg·s^{-1}·m^{-1}).

Nusselt numbers between 2 and 10, and inducing modified Grashof numbers between 1.5×10^6 and 1.5×10^7. In Fig. 7 describing the influence of the heat flux $\dot{q}_f$ imposed to the heated wall, the different plots show that the mass flow rate of evaporation as well as the temperature of the film increase with the heat flux. The mean specific mass flow rate of evaporation defined by

$$\bar{\dot{m}}_v = \frac{1}{h} \int_0^h \dot{m}_v(y)\,\mathrm{d}y \tag{26}$$

increases with $\dot{q}_f$. In the range from 200 W·m^{-2} to 1400 W·m^{-2}, the deviation observed between the plots of $\dot{m}_v$ is very sensitive, demonstrating that $\dot{q}_f$ plays a crucial role in the evaporation of the film. Furthermore, each of these temperature plots presents a linear part whose slope increases with the heat flux. This linearity which characterizes the absence of evaporation as well as the change of the slope with respect to $\dot{q}_f$ can be explained by Eq. (25). The influence of this parameter is better shown by the plot of variation of S_v (Fig. 7). The surface of evaporation increases with the heat flux. This variation is very noticeable for the lower values

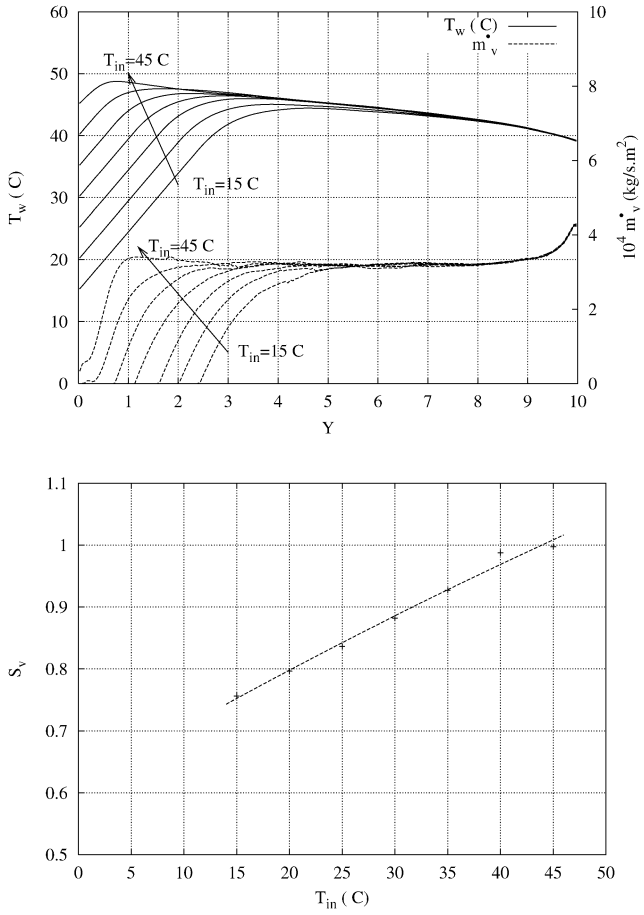

Fig. 8. Influence of the temperature of water feed. Top: profiles of film temperature and evaporated mass flux. Bottom: variation of the fraction of effective evaporation area (conditions: $T_c = 15\,^{\circ}\mathrm{C}$, $\dot{m}_{\mathrm{in}} = 0.808 \times 10^{-3}\ \mathrm{kg{\cdot}s^{-1}{\cdot}m^{-1}}$, $\dot{q}_f = 800\ \mathrm{W{\cdot}m^{-2}}$).

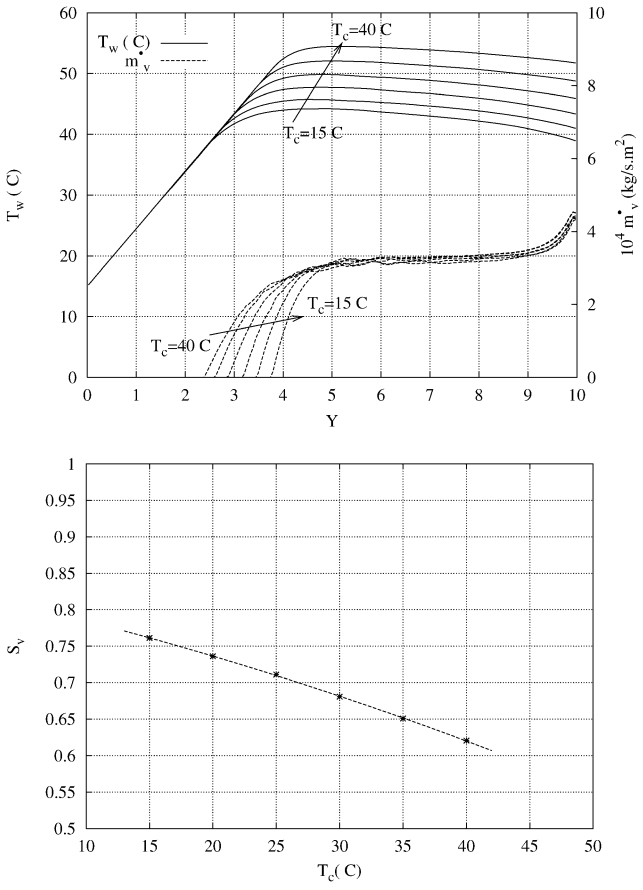

Fig. 9. Influence of the temperature of the condensation wall. Top: profiles of film temperature and evaporated mass flux. Bottom: variation of the fraction of effective evaporation area (conditions: $T_{\mathrm{in}} = 15\,^{\circ}\mathrm{C}$, $\dot{m}_{\mathrm{in}} = 0.808 \times 10^{-3}\ \mathrm{kg{\cdot}s^{-1}{\cdot}m^{-1}}$, $\dot{q}_f = 800\ \mathrm{W{\cdot}m^{-2}}$).

of $\dot{q}_f$ and attenuated at high values. The parameter S_v remains always lower than 0.8 even for large values of $\dot{q}_f$. This is due to the fact that the temperature of the feed water is low (15 °C) and that the film always presents a heating zone before evaporation begins.

8.2. Influence of the temperature of the feed water

The temperature of the feed water T_{in} represents a boundary condition and does not appear in expression (25). Thus the slope $\mathrm{d}T_w/\mathrm{d}y$ remains constant when T_{in} changes, which explains the fact that the plots of the variation of the temperature of the liquid film are parallel in the linear part characterizing the absence of evaporation (Fig. 8). From a given value of Y, the plots of the temperature of the liquid film get closer and are merged in the bottom of the cavity. The same behaviour is observed for the plots representing the variations of the evaporated mass flux. This result shows that, at the bottom of the cell, the falling film reaches a similar state of thermodynamic equilibrium independent of the temperature of the feed water. The ratio of the evaporation surface increases nearly linearly with T_{in} (Fig. 8). When the temperature of the feed water reaches 40 °C, S_v becomes close to 1, which means that the evaporation spreads on the majority of the film surface. At this temperature, water begins to evaporate significantly nearly as soon as it enters the top of the cell. This can be explained by the existence of an important temperature deviation between the liquid film at 40 °C and the condensation wall maintained at 15 °C. A concentration gradient results which causes the change of state of the liquid from the top of the cavity.

8.3. Influence of the temperature of the condensation wall

The influence of the temperature of the condensation wall T_c is shown on the plots of Fig. 9. In the higher part of the film characterized by the absence of evaporation, moreover with the condensation being neglected, the liquid simply heats itself and its temperature mainly depends on the temperature of the feed water and on the heat flux, which explains the common part of the curves corresponding to the different values of T_c. The influence of this parameter is essentially demonstrated in the evaporation zone. When T_c increases, the mean specific mass flow rate of evaporation decreases, as the rate of evaporation varies in the same

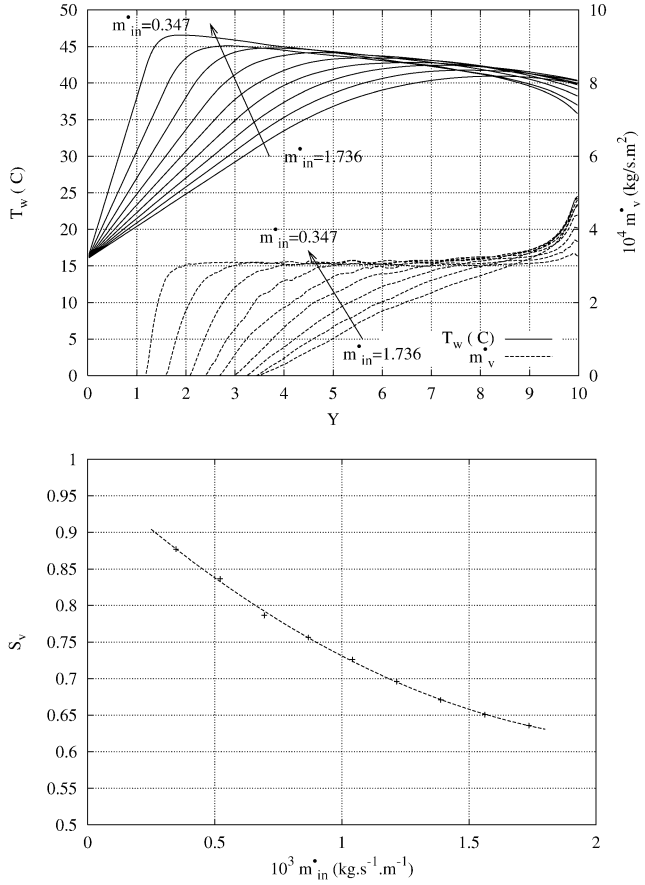

Fig. 10. Influence of the feed flow rate expressed in 10^{-3} kg·s^{-1}·m^{-1}. Top: profiles of film temperature and evaporated mass flux. Bottom: variation of the fraction of effective evaporation area (conditions: $T_c = 16\,^{\circ}$C, $T_{\text{in}} = 15\,^{\circ}$C, $\dot{q}_f = 800$ W·m^{-2}).

way as the temperature gradient which is reduced by an increase of the temperature of the condensation wall. Fig. 9 confirms the result that the fraction of the actual evaporation decreases when the value of the temperature of the condensation wall is increased.

8.4. Influence of the flow rate of feed water

The influence of the mass flow rate of feed water $\dot{m}_{\text{in}}$ on the evaporation of the film is shown on Fig. 10. The comparison of the plots relative to $\dot{m}_{\text{in}} = 3.47 \times 10^{-4}$ kg·s^{-1}·m^{-1} and $\dot{m}_{\text{in}} = 1.736 \times 10^{-3}$ kg·s^{-1}·m^{-1} shows that this parameter acts not only on the mean specific mass flow rate of evaporation, but also on the allure of the curve of the evaporation rate. This noticeable influence is explained by the importance of the sensitive heat evacuated by the falling liquid. This heat convected by the liquid increases with the flow rate of the liquid and consequently with the feed flow rate of the film. The more the feed flow rate is increased, the more the heat that can be transformed into latent heat is reduced. The feed flow rate influences also the extent of the effective surface of evaporation. When $\dot{m}_{\text{in}}$ increases, S_v decreases. This change is more sensitive for low values of the feed flow rate (Fig. 10). In order to promote evaporation, the user should work at low feed flow rates.

8.5. Characterization of heat and mass transfer

In order to generalize our results, the heat and mass transfer in the cavity have been described in terms of dimensionless numbers. The heat flux exchanged at the interface between the liquid film and the fluid inside the cavity results [1,21] as the sum of the convection and the latent contributions

$$\dot{q}_\delta = \dot{q}_{\text{cv}} + \dot{q}_l \tag{27}$$

Thus the local Nusselt number at the interface defined as

$$Nu_\delta = \frac{\dot{q}_\delta}{\dot{q}_{\text{cd}}} = \frac{\dot{q}_\delta b}{\lambda_g (T_{mw} - T_c)} \tag{28}$$

can be decomposed as

$$Nu_\delta = Nu_s + Nu_l \tag{29}$$

where Nu_s and Nu_l denote the Nusselt numbers relative respectively to the sensitive heat and the latent heat associated to evaporation [22], which can be expressed as

$$Nu_s = \frac{\dot{q}_{\text{cv}} y}{\lambda_g (T_{w\delta} - T_c)} \tag{30}$$

and

$$Nu_l = \frac{\dot{m}_v b L_v}{\lambda_g (T_{w\delta} - T_c)} \tag{31}$$

To describe the mass transfer, a local Sherwood number defined previously by [1] is used

$$Sh_l = \frac{\dot{m}_v (1 - w_\delta) b}{\rho_g (w_\delta - w_c) D} \tag{32}$$

In the definition of these dimensionless numbers, by analogy with pure convection without change of phase in cavities, the characteristic length is the cell width b. To characterize the heat and mass transfer associated with film evaporation, local Nusselt and Sherwood numbers are calculated along the interface. As shown previously, the evaporation of film is influenced by four parameters: the feed flowrate and temperature, the heat flux and the condensation temperature. However, in practice, these two latter parameters are generally fixed by the climatic conditions. The two first ones at the feed influencing the state of liquid film can be varied by the user. Their influence on the distribution of the dimensionless numbers has been studied.

The influences of the feed flow rate on the local Sherwood and Nusselt numbers have been studied in the zone of evaporation and are displayed on Fig. 11. At a given height, the evaporation starts and the local Nusselt and Sherwood numbers first increase nearly linearly with a decreasing slope when the feed flow rate increases. At low feed flow rates, the Nusselt and Sherwood numbers increase very slowly on a large part of the total surface. Close to the exit, a new increase of the Nusselt and Sherwood numbers appears. It is

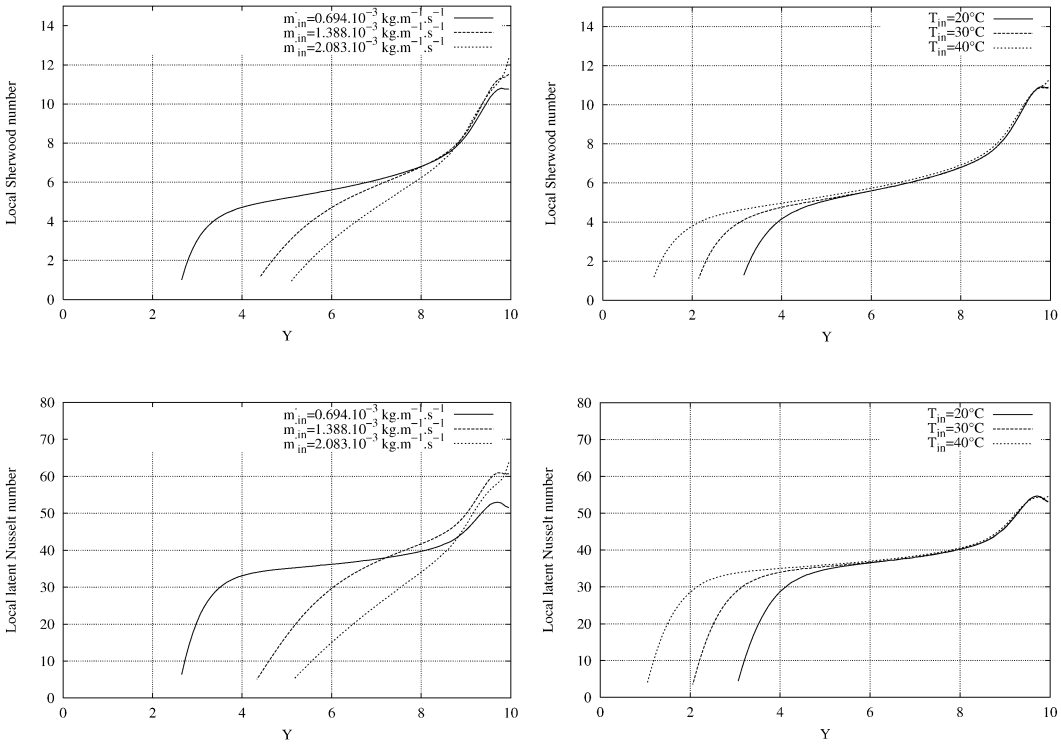

Fig. 11. Influence of feed flow rate (left: conditions: $T_c = 15\,^{\circ}\mathrm{C}$, $T_{\mathrm{in}} = 20\,^{\circ}\mathrm{C}$, $\dot{q}_f = 800\ \mathrm{W{\cdot}m^{-2}}$) and temperature (right: conditions: $T_c = 15\,^{\circ}\mathrm{C}$, $\dot{m}_{\mathrm{in}} = 0.833 \times 10^{-3}\ \mathrm{kg{\cdot}s^{-1}{\cdot}m^{-1}}$, $\dot{q}_f = 800\ \mathrm{W{\cdot}m^{-2}}$) on the local Sherwood (top) and Nusselt (bottom) numbers versus the dimensionless height.

probably due to the condition of adiabaticity at the lower side of the cell.

In a same way, the influence of feed temperature on the local Sherwood and Nusselt numbers is represented on Fig. 11. The characteristics of the curves presents similarities with those concerning the influence of the feed flow rate. In the evaporation zone, the local Sherwood and Nusselt numbers increase almost linearly with the same slope, then reach a level that extends on a large domain and does not depend on the feed temperature. Only the extent of the evaporation area increases with the feed temperature. Again, close to the exit, the local Sherwood and Nusselt numbers increase for the same reason as previously discussed.

8.6. Discussion

The numerical results show that, from the inlet of the cell, the temperature of the film first increases linearly until evaporation starts. Then the temperature ceases to increase and the received heat flux is transformed into latent heat. This result is in agreement with Mezaache and Daguenet [13] who studied the evaporation of a liquid film falling on an inclined plate. The small decrease of the temperature noted at the bottom of the cavity is caused by the intensification of evaporation. Near the top of cavity, the concentration of the gas mixture is relatively important (Ben Jabrallah et al. [16]). Due to the presence of liquid film in general colder close to the top (low T_{in}), a part of this vapor can condense on the wet surface. The calculation method in use can return account of

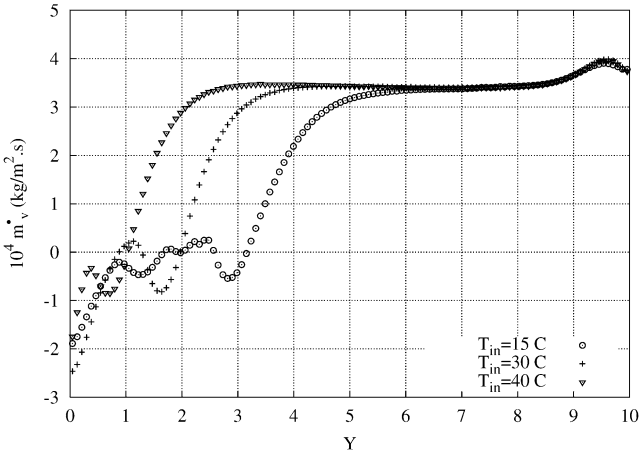

Fig. 12. Evidence of condensation of the vapor on liquid film at different water feed temperatures (conditions: $T_c = 16\,^{\circ}\mathrm{C}$, $T_{\mathrm{in}} = 15$, 30 and $40\,^{\circ}\mathrm{C}$, $\dot{m}_{\mathrm{in}} = 0.833 \times 10^{-3}\ \mathrm{kg{\cdot}s^{-1}{\cdot}m^{-1}}$, $\dot{q}_f = 800\ \mathrm{W{\cdot}m^{-2}}$).

this phenomenon. On Fig. 12, the mass flux of condensation on film corresponds to the part of the curve located at negative ordinates. The quantity of the vapor which condensates remains low and represents less than 7% of the total evaporated mass flux. However, the condensed part decreases as the inlet temperature of water increases. The assumption which consists in neglecting the condensation of the vapor on liquid film is then justified.

The method described in this work makes it possible to predict the heat flux consumed by evaporation. Fig. 13 describes the variation of the ratio of the latent heat flux of

evaporation to the total flux imposed on the wall. This ratio increases with the value of the flux imposed on the wall. Its variation is more marked for low values of $\dot{q}_f$ than for large values of $\dot{q}_f$ as the transfer of heat is then dominated by the transfer of latent heat to the interface. This result is in agreement with the conclusion of [1,3,9,10,13,18,21,23,24]. However, when the heat flux imposed on the wall is low, the greater part is carried as sensible heat flux by the liquid which heats up and the latent heat flux is then reduced. Eq. (15) rules the mass transfer between the surface and the gas phase. The direction of the mass transfer depends on the sign of the gradient of the saturated mass fraction w_{sat} at the interface. Thus, when the mass fraction at the interface is lower than the mass fraction inside the cavity, the mass transfer is directed towards the wetted surface and condensation of water vapor on the liquid film appears at the top of the cell. To better understand the favorable conditions to the appearance of this phenomenon, w_{sat} is presented along the wetted surface (Fig. 14), as well as the profiles of temperature and of the mass fraction w inside the cavity (Fig. 15). A similitude appears between the profiles of temperature and those of the mass fraction in the gas mixture. It can be explained by the analogy between the conservation equations respectively (6) and (7). The profiles of the mass fraction show that the gradient $(\frac{\partial w}{\partial x})_\delta$ is such that the transfer is performed in the evaporation direction on the main part of the wetted surface. The profiles at different levels are similar except for $Y = 1.25$ (near the top of the cell) where a recirculation of the gas mixture close to the top of the cavity [16] explains some condensation of water vapor on the liquid film.

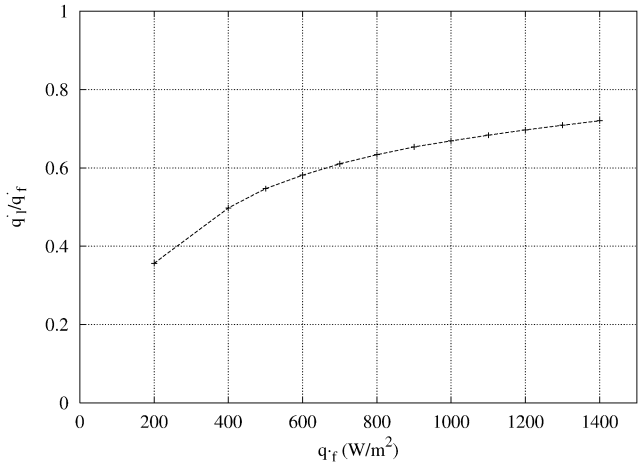

Fig. 13. Variation of ratio $\frac{\dot{q}_l}{\dot{q}_f}$ with respect to $\dot{q}_f$ (conditions: $T_c = 16\,^\circ\text{C}$, $T_{\text{in}} = 15\,^\circ\text{C}$, $\dot{m}_{\text{in}} = 0.833 \times 10^{-3}$ kg·s^{-1}·m^{-1}).

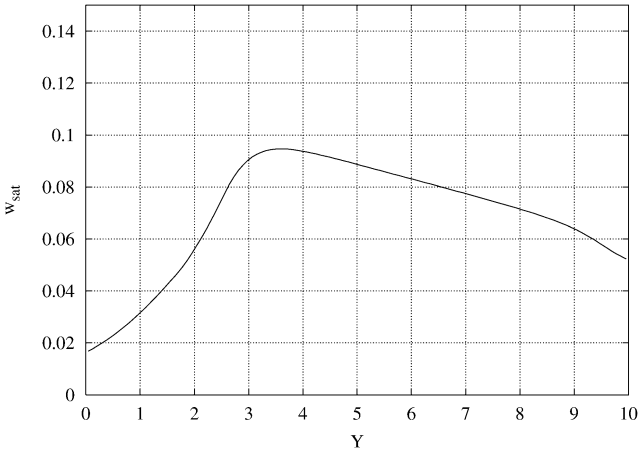

Fig. 14. Profile of saturated mass fraction along the height (conditions: $T_c = 15\,^\circ\text{C}$, $T_{\text{in}} = 20\,^\circ\text{C}$, $\dot{m}_{\text{in}} = 0.833 \times 10^{-3}$ kg·s^{-1}·m^{-1}, $\dot{q}_f = 800$ W·m^{-2}).

9. Conclusion

The present work concerned the study of the evaporation of a falling film in the case where the cell is a rectangular cavity whose wall bearing the liquid film is submitted to a constant heat flux, while the condensation wall is maintained at a given constant temperature.

A method of solving equations has been developed which holds account of the transfer in liquid film and also between the film and the surrounding gas. This method is based on integration of conservation equations, at a level y, to establish the local heat and mass balances. The solution of the

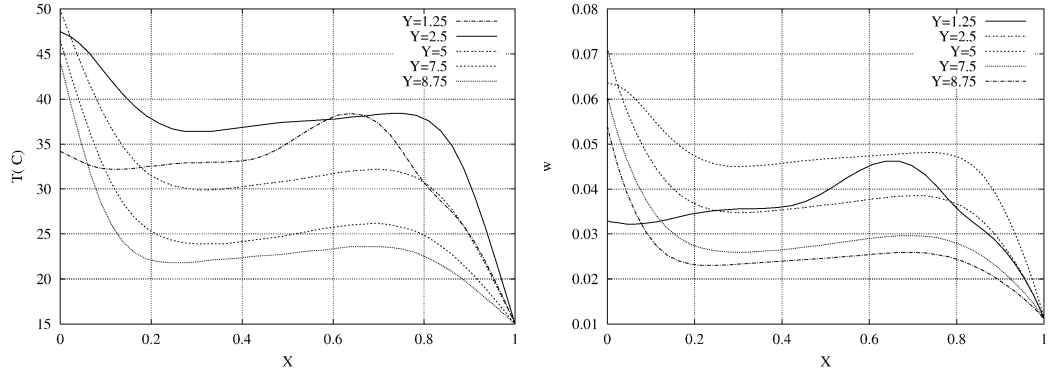

Fig. 15. Profiles of temperature (left) and mass fraction (right) in the gas phase at different heights (conditions: $T_c = 15\,^\circ\text{C}$, $T_{\text{in}} = 20\,^\circ\text{C}$, $\dot{m}_{\text{in}} = 0.833 \times 10^{-3}$ kg·s^{-1}·m^{-1}, $\dot{q}_f = 800$ W·m^{-2}).

balances in the liquid film coupled with the conservation equations in the gas phase allows us to describe the thermodynamic state of film by means of the temperature and the rate of evaporation at each level of the wet surface.

The effective surface of evaporation does not extend on the whole surface provided, but the film presents two zones: a heating zone for the liquid situated at the top of the heated wall, and an evaporation zone which extends on the remaining of the wetted surface. To characterize these two zones, the temperature and the rate of evaporation of the liquid film along the heated wall have been studied.

Four parameters related to the operating conditions mainly influence the thermodynamic state of the liquid film: on the one hand, the heat flux and the temperature of the condensation wall that in general depend on the climatic conditions, on the other hand, the water feed temperature and flow rate that can be varied by the user. It is shown that these parameters have an influence on the distribution of the temperature and on the evaporation rate of the film, but also on the extent of the evaporation surface. The influence of the feed parameters on the heat and mass transfer at the liquid–gas interface has been characterized by local Sherwood and Nusselt numbers. It is shown that the heat and mass transfer can be intensified by decreasing the feed mass flow rate, while an increase of the feed temperature does not increase the dimensionless numbers but increases the effective surface of evaporation.

References

[1] W.M. Yan, C.Y. Soong, Convective heat and mass transfer along an inclined heated plate with evaporation, Internat. J. Heat Mass Transfer 38 (1995) 1261–1269.
[2] W.M. Yan, T.F. Lin, Y.L. Tsay, Evaporative cooling of liquid film through interfacial heat and mass transfer in a vertical channel—I. Experimental study, Internat. J. Heat Mass Transfer 34 (1991) 1105–1111.
[3] W.M. Yan, T.F. Lin, Evaporative cooling of liquid film through interfacial heat and mass transfer in a vertical channel—II: Numerical study, Internat. J. Heat Mass Transfer 34 (1991) 1113–1124.
[4] C.J. Chang, T.F. Lin, W.M. Yan, Natural convection flows in a vertical, open tube resulting from combined buoyancy effects of thermal and mass diffusion, Internat. J. Heat Mass Transfer 29 (10) (1986) 1543–1552.
[5] L.C. Chow, J.N. Chung, Evaporation of water into a laminar stream of air and superheated stream, Internat. J. Heat Mass Transfer 26 (1983) 373–380.
[6] J. Schröppel, F. Thiele, On the calculation of momentum, heat and mass transfer in laminar and turbulent boundary layer flows along a vaporizing liquid film, Numer. Heat Transfer 6 (1983) 475–496.
[7] T.R. Shembharkar, B.R. Pai, Prediction of film cooling with a liquid coolant, Internat. J. Heat Mass Transfer 29 (1986) 899–908.
[8] W.W. Baumann, F. Thiele, Heat and mass transfer in evaporationg two-component liquid film flow, Internat. J. Heat Mass Transfer 33 (1990) 267–273.
[9] Y.L. Tsay, T.F. Lin, W.M. Yan, Cooling of falling liquid film through interfacial heat and mass transfer, Internat. J. Multiphase Flow 16 (1990) 853–865.
[10] W.M. Yan, T.F. Lin, Combined heat and mass transfer in natural convection between vertical parallel plates with film evaporation, Internat. J. Heat Mass Transfer 33 (1990) 529–541.
[11] A. Cherif, A. Daif, Etude numérique du transfert de chaleur et de masse entre deux plaques planes verticales en présence d'un film de liquide binaire ruisselant sur l'une des plaques chauffée, Internat. J. Heat Mass Transfer 42 (1999) 2399–2418.
[12] A. Agunaoun, A. Daif, R. Barriol, M. Daguenet, Evaporation en convection forcée d'un film mince s'écoulant en régime permanent, laminaire et sans ondes, sur une surface plane inclinée, Internat. J. Heat Mass Transfer 37 (18) (1994) 2947–2956.
[13] H. Mezaache, M. Daguenet, Etude numérique de l'évaporation dans un courant d'air humide laminaire d'un film d'eau ruissellant sur une plaque inclinée, Internat. J. Heat Thermal Sci. 39 (2000) 117–129.
[14] W. Nusselt, Die Oberflachenkondensation des Wasserdampfes, Z. Ver. Dt. Ing. 60 (1916) 541–546.
[15] W. Nusselt, Die Oberflachenkondensation des Wasserdampfes, Z. Ver. Dt. Ing. 60 (1916) 568–575.
[16] S. Ben Jabrallah, A. Belghith, J.P. Corriou, Etude des transferts couplés de matière et de chaleur dans une cavité rectangulaire: application à une cellule de distillation, Internat. J. Heat Mass Transfer 45 (2002) 891–904.
[17] C. Ouhaes, R. Ouhaes, P. Le Goff, Un distillateur multi-étagé à film capillaire, J. Internat. Thermique 2 (1987) 104–110.
[18] Y.L. Tsay, T.F. Lin, Evaporation of a heated falling liquid film into a laminar gas stream, Experimental Thermal Fluid Sci. 11 (1995) 61–71.
[19] S.V. Patankar, Numerical Heat Transfer and Fluid Flow, Hemisphere, New York, 1980.
[20] R.C. Reid, J.M. Prausnitz, B.E. Poling, The Properties of Gases and Liquids, McGraw-Hill, New York, 1987.
[21] A.G. Fedorov, R. Viskanta, A.A. Mohamad, Turbulent heat and mass transfer in asymmetrically heated, vertical parallel plate channel, Internat. J. Heat Fluid Flow 18 (3) (1997) 307–315.
[22] W.M. Yan, Effects of film vaporisation on turbulent mixed convection heat and mass transfer in a vertical channel, Internat. J. Heat Mass Transfer 38 (1995) 713–722.
[23] A. Agunaoun, A. Il Idrissi, A. Daïf, R. Barriol, Etude de l'évaporation en convection mixte d'un film liquide d'un mélange binaire s'écoulant sur une plaque inclinée soumise à un flux de chaleur constant, Internat. J. Heat Mass Transfer 41 (1998) 2197–2210.
[24] W.M. Yan, D. Lin, Heat and mass transfer in vertical annuli with film evaporation and condensation, Internat. J. Heat Mass Transfer 44 (2001) 1143–1151.